Implementation of Energy Efficient Single Switch Controlled SRM Drive

M.N.SaravanaKumar[1], R.Sreedhar[2]
[1]Research Scholar, Department of Electrical and Electronics Engineering, St Peter's University, Chennai, Tamilnadu, India
[2]Assistant Professor, Department of Electrical and Electronics Engineering, GGR college of Engineering, Vellore, Tamilnadu, India

Abstract

A low-cost and variable-speed drive requiring only a single controllable switch is presented. The proposed converter overcomes the drawback of the original single switch converter in terms of recovery energy circulation. The drive system is realized using an asymmetric two-phase switched reluctance motor (SRM), the proposed converter, and PIC controller. The new drive system retains the unique features of self-starting for all rotor position. A prototype drive has been built and tested to verify its practical viability. The market relevance of this new drive system is primarily due to its lowest cost structure, packaging compactness, self-starting feature and variable-speed operation. Because of these features, the new drive system offers a viable alternative to conventional fixed-speed brush-commutator motors and variable speed permanent magnet brushless dc motor drives in many high volume applications in the low-cost, energy efficient, high-volume categories such as fans, blowers, hand tools, and small appliances.

Keywords

Low-cost converter, switched reluctance motor (SRM), Variable-Speed drive.

1. Introduction

Environmental concerns and energy efficiency have increased demand for variable-speed drives in low-cost, low-performance, high-volume applications such as fans, hand tools and home appliances. Generally, most of these applications utilize constant-speed drives with throttling or damper control, leading to reduced efficiency and over-sized drive systems. They can benefit from variable-speed operation, delivering significant energy savings, higher reliability, and improved process control.

The conventional variable speed drives compared to fixed-speed drives has been the main reason for variable-speed drives which does not penetrated for such cost-sensitive applications. The switched reluctance motor (SRM) is known to be the lowest cost motor with the simplest construction having no brushes, commutators, windings, or magnets on its rotor and only concentrated windings on its stator. Converter for SRM had been made simple.

In the original converter, the recovered energy from the main winding stored in the recovery capacitor is circulated back to the dc-link capacitor, whereas in the new converter, the recovered energy from the main winding is retained and utilized within the motor instead of returning back to the source.

A single-phase SRM with a two-switch-based asymmetric converter and a two-phase SRM with two-switch-based split supply converter are found to be competitive for low-cost variable-speed applications. While these drives provide desirable performance with reduction in cost and component count would be highly appealing to some sect industries while for many others it is almost a necessity to meet highly cost sensitive high-volume applications.

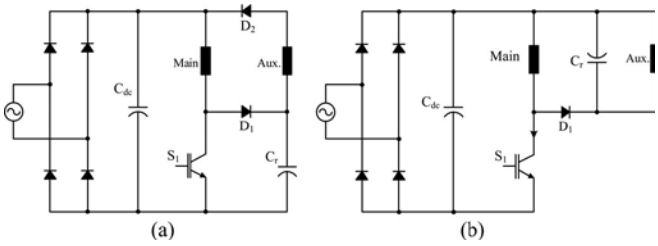

Fig. 1. Single-controllable-switch converters: (a) Original. (b) New.

The original and new single-controllable-switch-converter is shown in fig 1. The main fundamental difference that lies in recovery energy circulation. In the original converter, the recovered energy from the main winding stored in the recovery capacitor is circulated back to the dc link capacitor, whereas in the new converter, the recovered energy from the main winding is retained and utilized within the motor instead of being returned to the source. The energy

circulation between the motor and source can cause extra losses and result in a need for a larger dc link capacitor and it reduces the lifetime. This project presents the operation of the new converter coupled with the SRM and the design consideration for optimal commutation in single-pulse mode and comparison with other conventional converters and the new converter, followed by simulation and experimental verification in the subsequent sections.

2. Objective

To design, simulate and implement the single switch controlled SRM drive

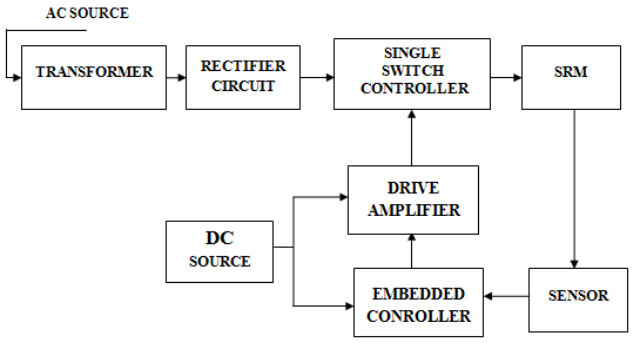

Fig. 2. Block diagram of single switch controlled SRM drive

3. Analysis of proposed circuit

The proposed converter shown in fig. 1 (b) has only one controllable switch and one diode, making the drive electronics very compact and inexpensive. Thus, it requires little PCB footprint. The motor employed in the proposed converter has asymmetric two-phase windings. (i.e. main winding for main torque production, auxiliary winding for self-starting and speed reversal)

The key features of the new drive system are described as follows:

1) A bridge rectifier with a filter capacitor C_{dc} forms a dc link to supply energy to the main phase winding.

2) Isolation for the gate drive circuit can be avoided since the switch S1 is tied with the negative dc rail.

3) The converters are inherently suited for two-phase SRMs having asymmetric stator phases to realize self- starting as well as speed reversal.

4) The recovery capacitor Cr along with the auxiliary winding is for handling recovery energy from the main phase. During the commutation of the main phase current, the current flows to charge Cr and to a small extent goes through the auxiliary winding.

5) During the main phase commutation, in the original converter shown in figure 1(a), -(*vCr* –*Vdc*) appears across the main winding resulting in the capacitor voltage *vCr* being maintained in the range of 1.5-2 times *Vdc* ; however, in the new converter, the voltage across the main winding equals -*vCr*, resulting in *vCr* being much less than *Vdc*.

6) In the original converter, the recovered energy stored in Cr is returned back to the dc link capacitor and this energy exchange between the motor and source causes extra losses leading to a larger dc link capacitor and active device ratings. In the new converter, however, the recovered energy is retained and utilized within the motor windings instead of being returned to the source.

7) Commutation time, a critical operation/control variable, is dependent on the size of Cr as well as the parameters of the main and auxiliary phases, as both phases are tightly coupled with Cr during the commutation. Therefore, optimal selection of Cr as well as auxiliary winding parameters is of prime importance for successful commutation of each phase current.

A. Modes of Operation

After properly understanding the operation of the converter coupled with the motor it is found that it is crucial to design and control of the drive system. From evaluation of all the possible combinations of the switching states of the switch and the diode, as well as the current commutation, five meaningful modes of operations emerge as illustrated in fig. 3((a) – (e)). The descriptions for each mode are discussed in the following and summarized in Table I.

MODE 1: When S1 is turned on, the main winding is energized with energy from the dc link. The auxiliary winding is also energized from Cr if there is a charge in Cr.

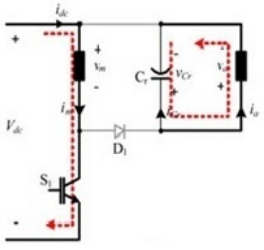

Fig. 3 (a). Mode 1 Operation

Mode 2: When S1 is still turned on, the main winding continues to be energized. If Cr is completely discharged,

then there is no current flow between Cr and the auxiliary winding.

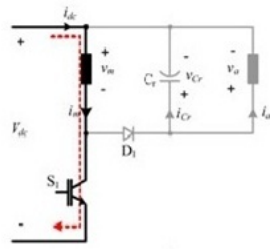

Fig. 3 (b). Mode 2 Operation

Mode 3: When S1 is turned off, the current in main winding flows through D1 and Cr as well as the auxiliary phase, hence transferring energy in part to Cr and in part to auxiliary winding.

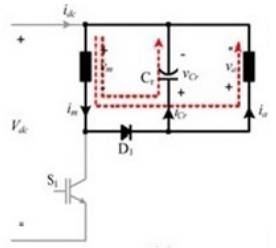

Fig. 3 (c). Mode 3 Operation

Mode 4: When S1 is turned off, both the main winding current and Cr supply the auxiliary winding.

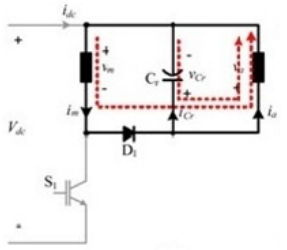

Fig. 3 (d). Mode 4 Operation

Mode 5: When S1 is turned off, and the main winding is successfully commutated, and Cr exclusively supplies the auxiliary winding current.

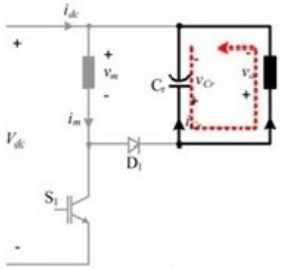

Fig. 3 (e). Mode 5 Operation

Table I Summary of modes of operation

Mode	S1	D1	i_{dc}	i_m	i_a	i_{Cr}	v_m	v_a
1	On	Off	>0	>0	>0	<0	V_{dc}	v_{Cr}
2	On	Off	>0	>0	=0	=0	V_{dc}	0
3	Off	On	=0	>0	>0	>0	$-v_{Cr}$	v_{Cr}
4	Off	On	=0	>0	>0	<0	$-v_{Cr}$	v_{Cr}
5	Off	Off	=0	=0	>0	<0	$-v_{Cr}$	v_{Cr}

4. Derivation of System Equations

The Drive system equations are derived in this section. The analytic modeling of each converter is obtained based on the state of the switch S1 (S=0(off), =1(on)) that the dc link and the power devices are assumed to be ideal; hence, the dc link voltage is constant and the device voltage drops are ignored for simplicity. The state equations for main and auxiliary phases as well as the capacitor Cr are given by

$$\frac{d\lambda_m}{dt} = \overbrace{S(V_{dc} - R_m i_m)}^{S_1\ ON} + \overbrace{(1-S)(-V_{cr} - R_m i_m)}^{S_1\ OFF} \quad (1)$$

$$\frac{d\lambda_a}{dt} = V_{cr} - R_a i_a \quad (2)$$

$$\frac{dV_{cr}}{dt} = \frac{i_{cr}}{C_r} = \frac{(1-S)i_m - i_a}{C_r} \quad (3)$$

$$i_{S1} = S i_m,\ i_{D1} = (1-S) i_m,\ i_{dc} = i_{S1} = S i_m \quad (4)$$

where λm and λa are the main and auxiliary phase flux linkages, im and ia are main and auxiliary phase currents, *Rm* and *Ra* are the main and auxiliary phase resistances, *Vdc* and *vCr* are the dc link and *Cr* voltages, respectively. The phase currents are obtained by mapping the flux linkage calculated from (1) and (2) to a lookup table of flux linkages in terms of current and rotor position. From the obtained phase currents, the currents for switch (*iS1*), diode (*iD1*), and dc link (*idc*) are also derived using the switching function as (4). The load dynamic equation of the motor is also given by

$$\frac{d\omega_r}{dt} = \frac{T_e - B\omega_r - T_L}{J} \quad (5)$$

where ω_r, T_e, T_L, J, and B are the rotor speed, electromagnetic torque, load torque, rotor and load inertia, friction coefficient, respectively.

5. Performance Constraints and Design Consideration

The design of the performance parameters for the converter based on the commutation time of the current and the

voltage rise in the recovery capacitor Cr due to the energy being transferred between the machine windings and the capacitor is explained below.

A. Commutation of Main and Auxiliary Phase Currents

The commutation of the main winding current is achieved through both the recovery capacitor and the auxiliary winding. In PWM operation, the voltage across the main winding switches back and forth between the positive (V_{dc}) and the negative voltage ($-V_{Cr}$). The current in the main winding also circulates through the auxiliary winding, transferring energy back and forth between the main and auxiliary winding resulting in continuous conduction of the auxiliary winding current. Although the net torque generated by the auxiliary phase is almost zero, current in the auxiliary winding during the main phase stroke generates negative torque, thus resulting in reduced efficiency and increased acoustic noise. This problem, however, can be eliminated if a voltage-fed, single-pulse control is employed. Although finer current control is not achievable with the single-pulse control, this is not a significant drawback since the target low performance fan type applications do not require finer current control. Furthermore, the motor will run mostly at top speed where single-pulse control is best suited. The optimal commutation in single-pulse mode is illustrated in figure 4, which shows the desired waveforms of main and auxiliary winding currents (i_m, i_a), and the voltage of the capacitor Cr (V_{Cr}).

When the switch S_1 is turned off at t_0, the main current flows through both C_r and the auxiliary winding. Thus, V_{Cr} and ia increases, which corresponds to mode 3. Once Cr is fully charged at t_1, Cr starts being discharged. Thus energy from both main winding and Cr is transferred to the auxiliary winding (mode 4). When the main winding current decays to zero at t_2, it is then only the capacitor that transfers energy to the auxiliary winding (mode 5). Therefore, it is more important to achieve the commutation such that both main and auxiliary winding currents fall to zero as soon as possible within the current stroke cycle (T_{ph}) to avoid negative torque generation.

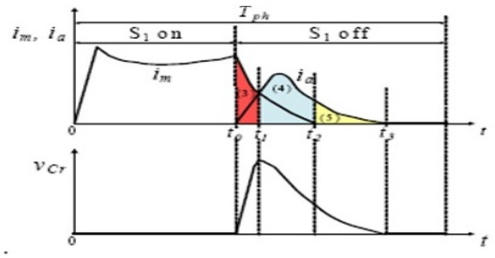

Fig. 4. Waveforms for the current commutation within a stroke cycle *T*ph in single-pulse mode.

B. Design Consideration for Optimal Commutation

The commutation time is highly dependent on the parameters (resistance and inductance) of both main and auxiliary windings as well as the size of Cr. Assume that the main phase is optimally designed for the machine power specification, the key design parameters are the size of Cr and the resistance and inductance of the auxiliary winding, which are determined mainly by the number of turns on a given machine structure. The calculation of the commutation time is as follows. The approximate voltage equation of an SRM phase is expressed as

$$\mathbf{V = Ri + L\frac{di}{dt} + i\frac{dL}{d\theta_r}\omega_r}$$

$$\mathbf{= \left[R + \omega_r\frac{dL}{d\theta_r}\right]i + L\frac{di}{dt}}$$

$$\mathbf{= R_{eq} + L\frac{di}{dt}} \qquad (6)$$

where *v*, *i*, *R*, *λ*, *L*, ω_r, θ_r, and R_{eq} are phase voltage, phase current, winding resistance, phase flux linkage, phase self inductance, rotor speed, rotor position, and equivalent phase resistance respectively. During commutation, the converter can be considered as an RLC circuit with the initial conditions. Therefore, the system equations for the equivalent RLC circuit are given by

$$\mathbf{R_{eqm}i_m + L_m\frac{di_m}{dt} = -V_{Cr}} \qquad (7)$$

$$\mathbf{R_{eqa}i_a + L_a\frac{di_a}{dt} = -V_{Cr}} \qquad (8)$$

$$\mathbf{C_r\frac{dV_{Cr}}{dt} = i_m - i_a} \qquad (9)$$

where R_{eqm} and R_{eqa} are the equivalent resistances for main and auxiliary windings, respectively, and *Lm* and *La* are the self-inductances of the main and auxiliary windings, respectively. The required commutation times (*t1*, *t2*, *t3*) as well as the peak voltage rise of Cr can be obtained by solving (7), (8), and (9) for $i_m(t)$, $i_a(t)$, and $V_{Cr}(t)$. However, solving the three simultaneous differential equations for an exact expression of i_m(t) is quite complecated. Therefore, by examining the piecewise waveforms in fig. 4 with an assumption that $i_m \approx i_{Cr}$ during the initial capacitor charging period, (7) can be rewritten as

$$\mathbf{R_{eqm}i_m + L_m\frac{di_m}{dt} + \frac{1}{C_r}\int i_m\,dt = 0} \qquad (10)$$

Then, the main winding current is derived as

$$i_m(t) = I_{m0}e^{-\alpha_m t}\cos\beta_m t + \left[\frac{V_{C0}}{\beta_m L_m} - \frac{\alpha_m I_{m0}}{\beta_m}\right]e^{-\alpha_m t}\sin\beta_m t \quad (11)$$

where

$$\alpha_m = \frac{R_{eqm}}{2L_m}, \beta_m = \sqrt{\frac{1}{L_m C_r} - \left(\frac{R_{eqm}}{2L_m}\right)^2} \quad (12)$$

I_{m0} is the initial current in the main winding at the beginning of commutation (t=to). During mode 3 region, the equation for the equivalent circuit between t_2 and t_3 can be expressed as

$$R_{eqa}i_a + L_a\frac{di_a}{dt} + \frac{1}{C_r}\int i_a\,dt + V_{C0} = 0 \quad (13)$$

Then, the auxiliary winding current is derived as

$$i_a(t) = I_{a0}e^{-\alpha_a t}\cos\beta_a t + \left[\frac{V_{C0}}{\beta_a L_a} - \frac{\alpha_a I_{a0}}{\beta_a}\right]e^{-\alpha_a t}\sin\beta_a t \quad (14)$$

where

$$\alpha_a = \frac{R_{eqa}}{2L_a}, \quad \beta_a = \sqrt{\frac{1}{L_a C_r} - \left(\frac{R_{eqa}}{2L_a}\right)^2} \quad (15)$$

I_{a0} is the initial current in the auxiliary winding at the beginning of commutation ($t = t_2$). The current commutation time for each winding current (t_{cm}, t_{ca}) is obtained by solving (11) and (14) using $i_m(t_{cm}) = 0$ and $i_a(t_{ca}) = 0$:

$$t_{cm} = \frac{\pi}{\beta_m} - \frac{1}{\beta_m}\tan^{-1}\left(I_{a0}/\left(\frac{V_{C0}}{\beta_m L_a} - \frac{\alpha_m I_{a0}}{\beta_m}\right)\right) \quad (16)$$

$$t_{ca} = \frac{\pi}{\beta_a} - \frac{1}{\beta_a}\tan^{-1}\left(I_{a0}/\left(\frac{V_{C0}}{\beta_a L_a} - \frac{\alpha_a I_{a0}}{\beta_a}\right)\right) \quad (17)$$

An approximate equation for C_r voltage is also obtained by solving (7), (8), and (9) for $V_{Cr}(t)$:

$$V_{Cr}(t) = \frac{I_{m0}\alpha+\gamma\beta}{C_r(\alpha^2+\beta^2)}\left\{1 - e^{-\alpha t}\cos\beta t + \frac{I_{m0}\beta - \gamma\alpha}{2}e^{-\alpha t}\cos\beta t\right. \quad (18)$$

where

$$\alpha = \sqrt{\frac{R_{eqm}+R_{eqa}}{C_r R_{eqa} L_a}} - \frac{R_{eqm}}{L_m}, \quad \gamma = \frac{V_{C0}}{\beta L_a} - \frac{\alpha I_{a0}}{\beta} \quad (19)$$

$$\beta = \sqrt{\frac{R_{eqm}+R_{eqa}}{C_r R_{eqa} L_a} - \left(\frac{L_m + L_a C_s R_{eqm} R_{eqa}}{2C_s R_{eqa} L_a}\right)^2} - \frac{R_{eqm}}{L_m} \quad (20)$$

The key parameters in the calculation of the commutation time from equation 16 and peak voltage ripple from equation 17 are the equivalent resistance and inductance of the winding and the capacitance of Cr. At constant speed, the equivalent resistance is mainly determined by the inductance slope, which in turn is determined by aligned and unaligned inductances with the rotor pole arc. For the current motor setup, the inductance of the auxiliary phase is varied by changing the number of turns. Therefore, the relationship between the inductance, capacitor and commutation time as well as the relationship between inductance, capacitor, and voltage ripple are investigated.

C. Comparison of Proposed converter with other converters

The comparison of the new single-switch converter with the original single-switch converter, the conventional asymmetric bridge converter for driving a single-phase motor and the full-wave bridge inverter for a three-phase ac machine is summarized in Table II

Table II Comparison of the new converter with other converters

Criteria	Full-wave Inverter	Asymmetric Bridge	Original Converter	New Converter
No. of power switches	6	2	1	1
No. of diodes	6	2	1	1
No. of gate drives	6	2	1	1
No. of power supplies for isolated gate drivers (min)	4	2	1	1
Switch voltage rating (min)	V_{dc}	V_{dc}	$2V_{dc}$	$2V_{dc}$
Switch current rating (peak)	I_p	I_p	I_p	I_p
Switch current rating (rms)	$I_p/\sqrt{3}$	$I_p/\sqrt{2}$	$I_p/\sqrt{2}$	$I_p/\sqrt{2}$
Converter VA rating (peak)	$6V_{dc}I_p$	$2V_{dc}I_p$	$2V_{dc}I_p$	$2V_{dc}I_p$
Switch conduction losses	$2d_sI_p$	$2d_sI_p$	d_sI_p	d_sI_p
Diode conduction losses	$2(1-d_s)I_p$	$2(1-d_s)I_p$	$(1-d_s)I_p$	$(1-d_s)I_p$
Recovery capacitor rating	N/A	N/A	$2.5V_{dc}$	$1.5V_{dc}$
Heat sink size (p.u)	2	1	0.5	0.5

Note: I_p is the peak rated motor phase current and d_s is the switch duty.

6. Simulation Circuit and Result

A. Open Loop Circuit of SRM drive

Figure below shows the open loop circuit diagram of single switch controlled SRM drive. The switch used in this circuit is MOSFET. The drive system consists of AC source, Diode bridge rectifier, dc link capacitor, MOSFET switch, recovery capacitor, and switched reluctance motor. Here, the AC source is converted into pulsating dc output and by means of dc link capacitor a ripple free dc output is obtained. The

performance of the motor is observed using scope block in MATLAB.

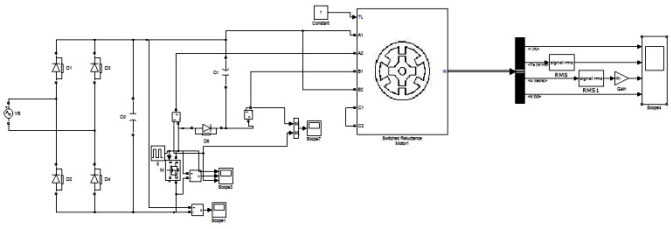

Fig. 5.1. Open loop simulation circuit for single switch controlled SRM drive

Fig. 5.2 depicts the input ac voltage of 150 V. This voltage fed to diode bridge rectifier and the 150 V ac voltage is converted into 150 V dc voltage and the ripples are reduced by properly adjusting the value of dc link capacitor.

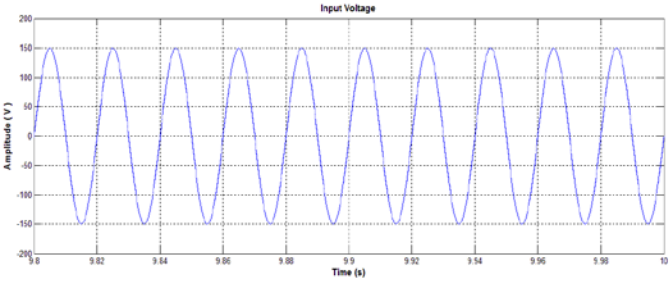

Fig. 5.2. Input voltage waveform

Fig. 5.3 depicts the MOSFET switching pulse for the switch M. The switch is turned on and off by applying gate pulse. These pulses are generated by pulse generator.

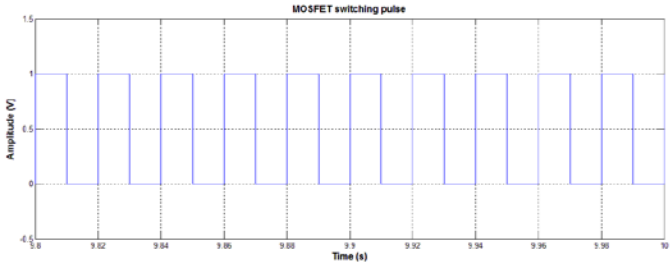

Fig. 5.3. MOSFET switching pulse

Fig. 5.4 depicts the current and voltage waveform of main and auxiliary winding and the torque- speed characteristics in open loop mode.

B. Closed loop circuit of SRM drive

Figure below shows the closed loop circuit diagram of single switch controlled SRM drive. The switch used in this circuit is MOSFET. The drive system consists of AC source, Diode bridge rectifier, dc link capacitor, MOSFET switch, recovery capacitor, and switched reluctance motor. Here, the AC source is converted into pulsating dc output and by means of dc link capacitor a ripple free dc output is obtained. The actual speed of the motor is compared with the set speed by means of a comparator and its output is given to the PI controller for generating pulse and then it is fed to the switch. The performance of the motor is observed using scope block in MATLAB.

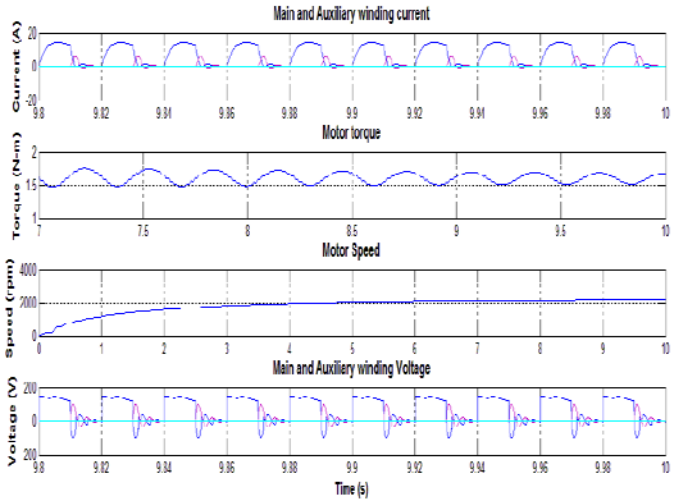

Fig. 5.4. Performance Characteristics of Two-phase SRM

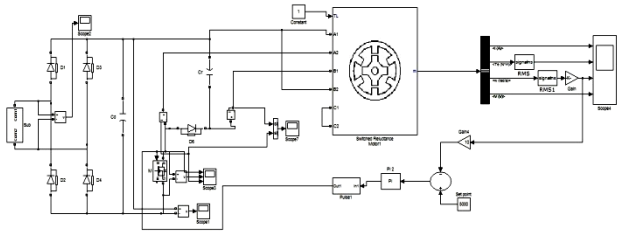

Fig. 5.5. Closed loop simulation circuit for single switch controlled SRM drive

Fig. 5.6 depicts the input ac voltage for the single switch controlled SRM drive.

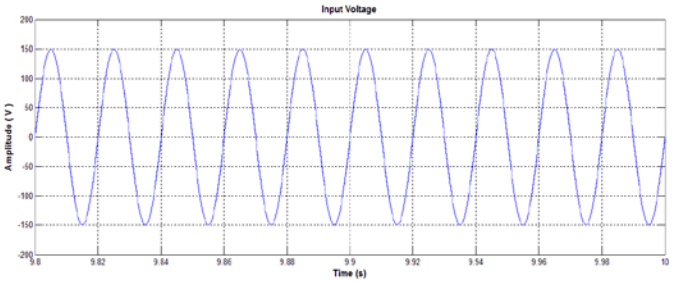

Fig. 5.6. Input voltage waveform

Fig. 5.7 depicts the MOSFET switching pulse for the switch M. The switch is turned on and off by applying gate pulse. These pulses are generated by pulse generator.

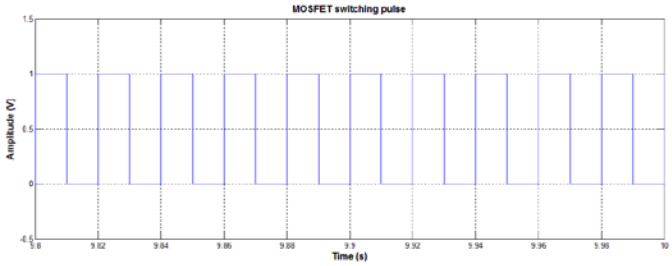

Fig. 5.7. MOSFET switching pulse

Fig. 5.8 depicts the current and voltage waveform of main and auxiliary winding and the torque- speed characteristics in closed loop mode.

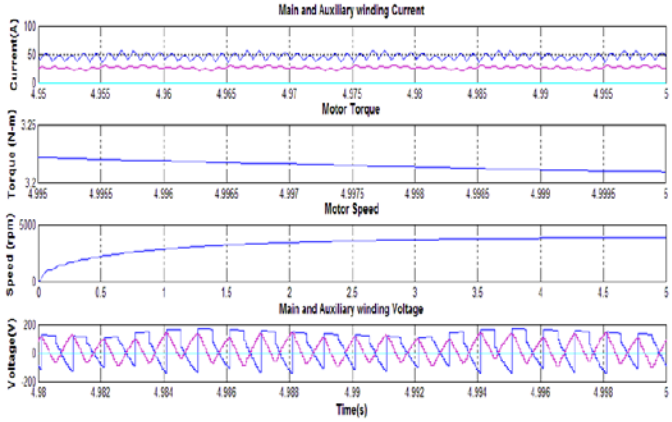

Fig. 5.8. Voltage, current, Torque and Speed waveform

7. Conclusion

The simulation of the module layout was successfully carried out using Matlab Simulink software and the obtained waveforms were observed.The output responses of the switched reluctance motor drive is analyzed.

A single switch controller is used to control the SRM drive. In general, each winding in SRM is controlled by separate switches. Apart from that, a single switch is going to control the main and auxiliary windings of the SRM. The proposed drive will have much impact in the future.

References

[1] Cao X., Deng Z., Yang G. and Wang X. (2009) 'Independent control of average torque and radial force in bearingless Switched Reluctance Motors with hybrid excitations' IEEE Transaction, Power Electronics, vol. 24, no. 5, pp. 1376 – 1385.

[2] Chang H.C. and Liaw C.M. (2008) 'On the front-end converter and its control for a battery powered Switched Reluctance Motor drive' IEEE Transaction Power Electronics, vol. 23, no. 4, pp. 2143–2156.

[3] Cheng and Liaw C.M. (2008) 'On the design of power circuit and control scheme for Switched Reluctance Generator' IEEE Transaction, Power Electronics, vol. 23, no. 1, pp. 445–454.

[4] Chomat M. and Lipo T.A. (2003) 'Adjustable-speed single-phase IM drive with reduced number of switches' IEEE Transaction, Industrial Application, vol. 39, no. 3, pp. 819–825.

[5] Krishnan R. (1997) 'A novel single-switch-per-phase converter topology for four-quadrant PM brushless DC motor drive' IEEE Transaction, Industrial Application, vol. 33, no. 5, pp. 1154–1161.

[6] Krishnan R., Park S.Y. and Ha K.S. (2005) 'Theory and operation of a four-quadrant switched reluctance motor drive with a single controllable switch-the lowest cost brushless motor drive' IEEE Transaction, IAS, vol. 41, no. 4, pp. 1047–1055.

[7] Welchko B. and Lipo T.A. (2001) 'A novel variable-frequency three-phase induction motor drive system using only three controlled switches' IEEE Transaction, Industrial Application, vol. 37, no. 6, pp. 1739–1745.

[8] Xue X.D., Cheng K.W.E. and Ho S.L. (2009) 'Optimization and evaluation of torque-sharing functions for torque ripple minimization in Switched Reluctance Motor drives' IEEE Transaction, Power Electronics, vol. 24, no. 9, pp. 2076–2090.

[9] Yang G., Deng Z., Cao X., and Wang X. (2008) 'Optimal winding arrangements of a bearingless Switched Reluctance Motor' IEEE Transaction. Power Electronics, vol. 23, no. 6, pp. 3056–3066.

Author's Profile

M N Saravana Kumar has received his Master of Engineering degree in Power Electronics and Drives from Rajalakshmi Engineering College, Chennai in the year 2013. At present he is pursuing Ph.D. with the specialization of Electrical Engineering in St. Peter's University. His area of interests are Power Electronics, Electro-magnetic Field and High Voltages.

R Sreedhar has received his Master of Engineering degree in Power Electronics and Drives from Kalasalingam University, Krishnankoil in the year of 2013. He received his bachelor degree in Electrical and Electronics Engineering from P.S.R Engineering college Sivakasi under Anna University Chennai. His area of interests are Power Electronics and Drives, Power System Analysis and Electrical Machines.